

Resorption-Cycle-dependent Polarization of mRNAs for Different Subunits of V-ATPase in Bone-resorbing Osteoclasts

Tiina Laitala-Leinonen,^{*†} Michael L. Howell,[‡] Gary E. Dean,[‡] and H. Kalervo Väänänen^{*}

^{*}Biocenter and Department of Anatomy, University of Oulu, Kajaanintie 52A, FIN-90220 Oulu, Finland; and [‡]Department of Molecular Genetics, Biochemistry and Microbiology, University of Cincinnati Medical Center, Cincinnati, Ohio 45267-0524

Submitted May 22, 1995; Accepted October 2, 1995
Monitoring Editor: Judith Kimble

Protein sorting in eukaryotic cells is mainly done by specific targeting of polypeptides. The present evidence from oocytes, neurons, and some other polarized cells suggests that protein sorting can be further facilitated by concentrating mRNAs to their corresponding subcellular areas. However, very little is known about the mechanism(s) involved in mRNA targeting, or how widespread and dynamic such mRNA sorting might be. In this study, we have used an *in vitro* cell culture system, where large multinucleated osteoclasts undergo continuous structural and functional changes from polarized (resorbing) to a nonpolarized (resting) stage. We demonstrate here, using a nonradioactive *in situ* hybridization technique and confocal microscopy, that mRNAs for several vacuolar H⁺-ATPase subunits change their localization and polarity in osteoclasts according to the resorption cycle, whereas mRNA for cytoplasmic carbonic anhydrase II is found diffusely located throughout the osteoclast during the whole resorption cycle. Antisense RNA against the 16-kDa or 60-kDa V-ATPase subunit inhibits polarization of the osteoclasts, as determined by cytoskeleton staining. Antisense RNA against carbonic anhydrase II, however, has no such effect.

INTRODUCTION

Post-translational sorting mechanisms for several different proteins are now well established, and allow targeting of specific proteins to their final destination in the cytoplasm. This process could be further facilitated by the proper localization of mRNA that could be done either by targeting the nascent polypeptide chain with mRNA, or by targeting the mRNA itself (Jackson and Standart, 1990; Jackson, 1993). The first evidence of polarized localization of specific mRNAs from oocytes (Berleth *et al.*, 1988; Yisraeli and Melton, 1988), and more recent observations from several other cells, has confirmed the specific concentration of certain mRNAs and their transcription products to distinct cytoplasmic areas (Trapp *et al.*, 1987; Garner *et al.*, 1988; Lawrence *et al.*, 1988; Macdonald and Struhl,

1988; Singer *et al.*, 1989). Concentration of mRNA and its corresponding protein to certain cytoplasmic areas in cells has been described in fibroblasts, epithelial cells, nerve cells, myoblasts, and endothelial cells (Gay and Mueller, 1974; Singer *et al.*, 1989; Hooek *et al.*, 1991; Sundell and Singer, 1991). In fibroblast cultures, specific cytoplasmic localization of actin mRNA suggests that mRNA can regulate its subcellular localization without protein synthesis (Hesketh and Pryme, 1991).

The evidence so far available about mRNA sorting in structurally and functionally polarized cells is scarce. By stimulating polarized cells apically, mRNA levels of apically secreted proteins increase (Wang *et al.*, 1991). In nerve cells, proteins and mRNAs are sorted into specific subcellular compartments during myelination (Trapp *et al.*, 1987).

Osteoclasts are multinuclear bone-resorbing cells that rapidly transform from an inactive, nonpolarized

† Corresponding author.

stage to an active, polarized stage (Lakkakorpi and Väänänen, 1991). Osteoclasts resorb bone by generating an acidic compartment between the bone surface and the bone-facing cell membrane called the ruffled border, which is especially rich in the vacuolar H⁺-ATPase¹ (V-ATPase; Blair *et al.*, 1989; Väänänen *et al.*, 1990). Protons, whose generation is facilitated by a cytoplasmic carbonic anhydrase II (CA II), are transferred across the ruffled border membrane by V-ATPase. It is a multisubunit enzyme, composed of independently assembled cytoplasmic (V₁) and membrane (V₀) domains (Doherty and Kane, 1993). The V₀ complex is highly hydrophobic and contains a 116-kDa subunit, and at least six copies of a 16-kDa subunit that form a proton channel. The V₁ domain contains three copies each of a 70-kDa and a 60-kDa subunit, along with subunits of 27, 32, 36, and 42 kDa. Of these, the 70-kDa subunits form the catalytic domain (Nelson, 1989). The function of the other subunits is unknown. The V-ATPase subunits from a number of species are highly homologous proteins found in vacuoles of yeast and different mammalian cells (Nelson *et al.*, 1994).

Both V-ATPase and CA II have a vital role in bone resorption, and inhibition of V-ATPase or CA II abolishes bone resorption (Hall and Kenny, 1987; Sundquist *et al.*, 1990; Laitala and Väänänen, 1994). We have studied the importance and distribution of mRNAs for CA II and different subunits of V-ATPase in cultured rat osteoclasts using an *in vitro* model that allows the normal polarization of osteoclasts. In this model, isolated rat osteoclasts are cultured on bovine bone slices, where they undergo resorption cycles and excavate distinct resorption pits (Lakkakorpi *et al.*, 1989; Lakkakorpi and Väänänen, 1990). After *in situ* hybridization, mRNAs can be detected with a confocal laser scanning microscope.

MATERIALS AND METHODS

All restriction enzymes were purchased from New England Biolabs (Beverly, MA), Life Technologies (Gaithersburg, MD), or Boehringer Mannheim GmbH (Mannheim, Germany). RNA-polymerases and DNA-modifying enzymes were purchased from Promega (Madison, WI) and Sequenase sequencing kits were purchased from United States Biochemical (Cleveland, OH). Other reagents were obtained from Sigma Chemical (St. Louis, MO).

Cloning of V-ATPase Subunits

Parts of the mouse 16-kDa, 31-kDa, 60-kDa, and 70-kDa V-ATPase subunit cDNAs were cloned by polymerase chain reaction (PCR) and sequenced to permit confirmation of their identity as V-ATPase subunits. These PCR fragments were then used to clone full-length cDNAs for each subunit. For the 16-kDa subunit, degenerate oligonucleotides designed to encode the predicted peptide sequence of bovine V-ATPase subunit c (Mandel *et al.*, 1988) at peptide positions

60–66 (BO16–5'A.082, sense orientation: GT[C/G]ATGGC[A/G/C]GG[C/G]AT[A/C/T]AT[A/C/T]GC) and peptide positions 128–133 (BO16–3'A.083, antisense orientation: AT[C/G]AG[A/G/T]AT-CAT[A/G/C]CC[C/G]AC [A/G]AA) were used. For the 31-kDa subunit, degenerate oligonucleotides designed to encode the predicted peptide sequence of the bovine V-ATPase subunit E (Hirsch *et al.*, 1988) at amino acid residues 23–28 (BO31–5'A, sense orientation: GC[C/T]AA[C/T] GAGAA[A/G]GC[A/C/T]GA[A/G]GA [A/G]AT) and residues 162–166 (BO31–3'A, antisense orientation: TC[A/G]AT[C/T]TG[A/G]AC[A/G]TCNAC[A/G]TC, where N=A/T/C/G) were used. For the 60-kDa subunit, degenerate oligonucleotides designed to encode the predicted peptide sequence of the *Arabidopsis thaliana* V-ATPase subunit B (Manolson *et al.*, 1988) at peptide positions 520–544 (GD2354, sense orientation: GGGGCGCC [I/C]CA[C/T]AA[C/T]GA[A/G]AT[T/C]GC[T/C]GC[I/C]C) and peptide positions 1012–1039 (GD2357, antisense orientation: TGC-GATCGGTGAT[A/G]TC[A/G]TC[A/G]TTNGGCAT) were used. Finally, for the 70-kDa subunit, degenerate oligonucleotides designed to encode the predicted peptide sequence of the bovine V-ATPase subunit A (Pan *et al.*, 1991) at positions 276–290 (GD2355, sense orientation: GGCGAGCTCGGNAA[C/T]GA[A/G]ATGGC-NGA[A/G]GT), and positions 431–449 (GD2356, antisense orientation: CTTGGCCAG[C/T]TT[C/T]TT[A/G]TCNA[A/G]NCC CCA) were used. Each set of primers was used in PCR reactions to amplify mouse subunit c cDNA from a mouse 18.5-day old embryoid body cDNA library in λ -gt11 (Pan *et al.*, 1991); the template in each reaction was 10 ng of purified λ -gt11 library DNA. The PCR reaction products were blunt-ended with T4 polymerase (Ausubel *et al.*, 1992), subcloned into pBluescript SK(–) (Stratagene, La Jolla, CA) at the *EcoRV* site, and their DNA sequences were determined. Promising inserts of 274 bp (16-kDa subunit), 437 bp (31-kDa subunit), 503 bp (60-kDa subunit), and 480 bp (70-kDa subunit) were in turn used to screen 4.6×10^5 plaques from the same library. Several of the longest clones obtained after several rounds of plaque purification for each subunit were excised with *EcoRI*, subcloned into pBluescript SK(–), and analyzed further. All DNA sequencing was performed on both strands by the dideoxy method as described (Ausubel *et al.*, 1992) on double-stranded plasmid DNA. Computer analysis was performed using DNANALYZ (Gregory Wernke, University of Cincinnati, Cincinnati, OH), and Clone and Align software from Scientific and Educational Software. The mouse 16-, 31-, 60-, and 70-kDa V-ATPase subunit cDNA sequences have been submitted to GenBank, and have been given the following accession numbers: U13842 (16 kDa), U13841 (31 kDa), U13838 (60 kDa), and U13837 (70 kDa).

In Vitro Transcription

The cloned PCR products were used as templates for *in vitro* transcription and probe synthesis. The length of the cloned cDNA-fragments varied between 220 bp (for the 16-kDa subunit) and 500 bp (for the 60-kDa subunit). Mouse CA II cDNA was obtained from Dr. Curtis (Wistar Instruments, Philadelphia, PA; Curtis *et al.*, 1983). Isolated cDNAs were labeled with fluorescein isothiocyanate (FITC)-dUTP using Klenow-enzyme (Sambrook *et al.*, 1989; Ausubel *et al.*, 1992). The resulting cDNA-probes were used for *in situ* hybridization. λ -DNA and γ -actin cDNA were used as control probes. For *in vitro* transcription, plasmids containing the 16-kDa or 60-kDa V-ATPase cDNAs or CA II cDNA were linearized with *EcoRI* or *BamHI*. RNA was transcribed *in vitro* using T3 or T7 RNA polymerase according to Promega's instructions, to obtain both the sense and antisense RNA-strands. RNA molecules were used at 1 μ g/ml concentrations. Fifty units of rRNasin/ml (Promega) was added to the culture medium 15 min before adding the RNA, to inactivate RNase activity in the medium. Samples with no nucleotide addition or with sense-RNA were used as controls.

¹ Abbreviations used: CA II, carbonic anhydrase II; dbcAMP, dibutyryl cyclic AMP; V-ATPase, vacuolar-type H⁺-ATPase.

Osteoclast Culture

Osteoclasts from 2- to 3-day old Sprague-Dawley rat long bones were scraped into DMEM (Life Technologies, Paisley, UK), and seeded onto bovine cortical bone slices as previously described (Lakkakorpi *et al.*, 1989; Laitala and Väänänen 1994). After 30 min, nonattached cells were washed away, and cells were cultured at 37°C (5% CO₂, 95% air) for 20 min or 24 h in the presence of 1 nM or 10 nM bafilomycin A₁, vehicle, 25 μM colchisin, 20 μM cytochalasin B (Serva, Heidelberg, Germany), 1 mM dibutyryl cAMP (db-cAMP), or 1 μg of antisense, sense, or scrambled RNA/ml. A total of 250 osteoclasts were studied in each experiment; osteoclasts were regarded as cells with at least three nuclei. Samples were viewed in a confocal laser scanning microscope consisting of a 750 mW air-cooled argon laser (Omnichrome, Chino, CA), a Leitz Aristoplan microscope, and 1.05-software (Leica Lasertechnik GmbH, Heidelberg, Germany). Scanning was performed in both XY- and XZ-planes using a 63× objective, a 128 pinhole, a 0.5-μm step size, and 256 × 256 pixel images. Resorption activity of each osteoclast was determined by nonconfocal transmission illumination that allowed visualization of the resorption lacunas under the osteoclasts.

In Situ Hybridization and Immunostaining

Before hybridization with fluorescein(FITC)-labeled cDNA as described before (Laitala and Väänänen, 1993), cells were fixed with buffered formaline (pH 7.4), and permeabilized for 5 min with 0.5% Triton at 0°C. Detection of CA II protein with polyclonal CA II antibodies (Sundquist *et al.*, 1987) and rhodamine(TRITC)-conjugated swine anti-rabbit Igs (Dakopatts A/S, Glostrup, Denmark) was performed before hybridization. Nonspecific binding of antibodies was blocked with 3% bovine serum albumin (BSA) (37°C, 30 min) before incubating the samples with the 1:100-diluted CA II antibody in 0.5% BSA (37°C, 30 min). Excess antibody was removed by washing the samples in phosphate-buffered saline (PBS), and TRITC-conjugated secondary antibodies (1:100) were added in 0.5% BSA. After 30 min at 37°C, samples were washed with PBS, and transferred to prehybridization. To enhance hybridization, 1% dextran sulfate was added to the standard prehybridization mixture (Laitala and Väänänen, 1993). Prehybridization was performed at 39°C (3 h), and hybridization was started by adding 500 ng of FITC-labeled probe per milliliter. After hybridization overnight at 39°C, nuclei were rapidly stained with 10 nM propidium iodide, and samples were embedded in Vectashield (Vector Laboratories, Burlingame, CA).

Northern Hybridization

Northern hybridizations from cultures treated with bafilomycin A₁ were done to quantitate the 16-kDa V-ATPase subunit mRNA levels in these samples. Also, the effects of antisense, sense, and scrambled RNA were studied using Northern blots. Six bone slices were pooled for each mRNA isolation, and ³²P-labeled cDNA probes were used in the hybridizations (Laitala and Väänänen, 1993).

Polarity of Osteoclasts

To study the activity and polarization of osteoclasts, the specific arrangement of F-actin in resorbing osteoclasts was studied (Lakkakorpi *et al.*, 1989; Lakkakorpi and Väänänen, 1990, 1991). Actin rings were visualized in the cultures with 5 U of FITC or TRITC-conjugated phalloidin per milliliter (Molecular Probes, Eugene, OR). Microtubules were stained using a 1:200-diluted monoclonal anti-α-tubulin antibody (Sigma) and TRITC-conjugated secondary antibodies (Dakopatts). Resorption lacunas were stained with peroxidase-conjugated WGA-lectin, as previously described (Selander *et al.*, 1994). A MCID/M2 image analyzer (Imaging Research, Brock University, Ontario, Canada) was used to count the areas of the resorption lacunas, and statistical significancies were determined by Student's *t*-test and variance analysis.

Western Blotting

Osteoclasts cultured on bone slices with antisense, sense, or scrambled RNA were used for Western blotting to further confirm the specificity of these antisense RNAs to inhibit translation. After culturing the osteoclasts on bone slices for 24 h, cells were washed with PBS and total proteins were isolated as described (Laitala and Väänänen 1994). A polyclonal CA II antibody and a polyclonal antibody against the 60-kDa subunit of V-ATPase from human brain were used in the experiment. HRP-conjugated secondary antibodies (Bio-Rad, Richmond, CA) were added, and antibodies were detected by chemiluminescence using a kit from DuPont NEN (Boston, MA).

RESULTS

Cloning and Analysis of cDNAs Encoding the Mouse V-ATPase Subunits

Sixty-seven clones for subunit A, 35 clones for subunit B, and 26 clones for subunit E were identified in the screening for the mouse V-ATPase subunit cDNAs. One of the longest clones (70–1, subunit A; 60–13, subunit B; and 31–39, subunit E) was selected from each subunit for further analysis and the cDNA insert sequences, presented in Figure 1, were determined. The positions of the original PCR products are shown by underlining.

The mouse subunit A protein sequence is predicted to begin at nucleotide number 19 and terminate at nucleotide number 1869, resulting in a 617-residue protein with a calculated molecular mass of 68,190 kDa and a predicted pI of 5.46. A comparison of the mouse peptide sequence with subunit A protein sequences from *B. taurus* (Pan *et al.*, 1991; Pupolo *et al.*, 1991), *Daucus carota* (Zimniak *et al.*, 1988), *Saccharomyces cerevisiae* minus the intein (Shih *et al.*, 1988; Hirata *et al.*, 1990), *Candida tropicalis*, also lacking the intein (Gu *et al.*, 1993), and *Neurospora crassa* (Bowman *et al.*, 1988b) show that the sequences have identities of 98.1, 68.7, 64.7, 64, and 62.7%, respectively, indicating that the sequence of this protein is highly conserved.

The mouse 60-kDa subunit protein sequence is predicted to begin at nucleotide number 15 in the sequence, and terminate at nucleotide number 1547, resulting in a 511-residue protein that would have a calculated molecular mass of 56,520 kDa, and a predicted pI of 5.41. A comparison of the mouse peptide sequence with those of bovine-1 (Pan *et al.*, 1993), *S. cerevisiae* (Nelson *et al.*, 1989), *Arabidopsis thaliana* (Manolson *et al.*, 1988), and *N. crassa* (Bowman *et al.*, 1988a) show that the sequences have identities of 96.9, 73.4, 72.1, and 72.0%, respectively, indicating that the sequence of this protein is highly conserved, as has been previously noted.

The mouse 31-kDa subunit protein sequence is predicted to begin at nucleotide number 66 in the sequence, and terminate at nucleotide number 749, resulting in a 228-residue protein that would have a calculated molecular mass of 26,557 kDa and a pre-

dicted pI of 9.82. A comparison of the mouse peptide sequence with those of the human (van Hille *et al.*, 1993b), *B. taurus* (Hirsch *et al.*, 1988), and *S. cerevisiae* (Foury, 1990) show protein sequence identities of 93.5, 93.5, and 33.2%.

The sequence for the mouse 16-kDa subunit agrees precisely with that already published (Hanada *et al.*, 1991). The PCR product for the 16-kDa subunit spans the region between nucleotides 340 and 530 of the previously reported sequence.

RNA Analysis and In Situ Hybridization

Previous immunohistochemical studies have shown that the V-ATPase in osteoclasts is mainly located in the bone-facing ruffled border membrane (Blair *et*

al., 1989; Väänänen *et al.*, 1990). We wished to use our mouse cDNA probes for in situ localization studies with rat cellular mRNA. As shown in Figure 2, each of our PCR-amplified cDNA fragments specifically hybridized with a single species of mRNA in Northern blots. In situ hybridizations clearly showed that mRNA for the 16-kDa V-ATPase subunit was also polarized to the perinuclear areas between the lowest nuclei and bone surface in resorbing osteoclasts (Figure 3, a–d). In contrast, the mRNA for CA II was diffusely distributed throughout the whole cytoplasm of resorbing osteoclasts (Figure 3, e–h). Immunostaining with anti-CA II antibody also revealed a diffuse distribution of this protein (Figure 3, i–j), and simultaneous staining for

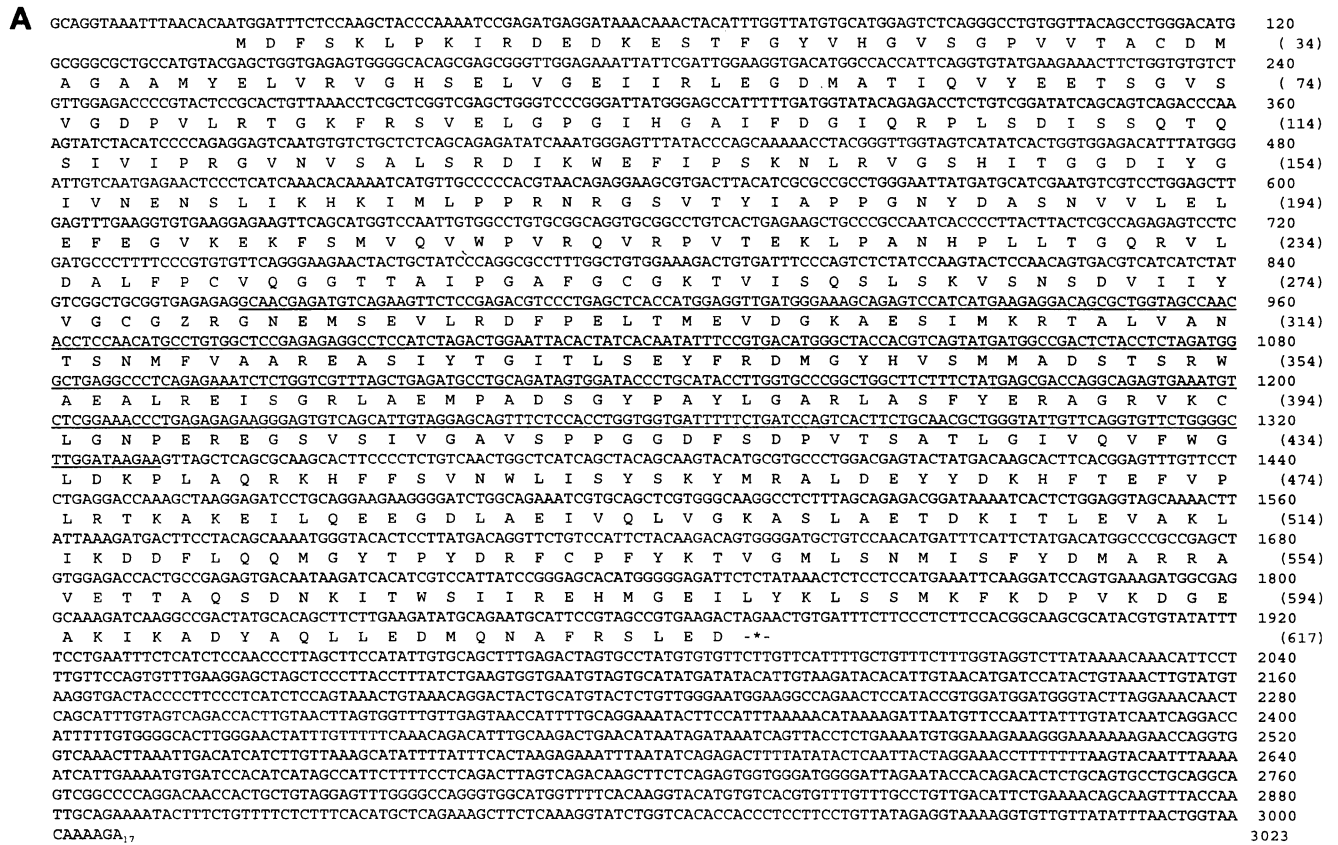
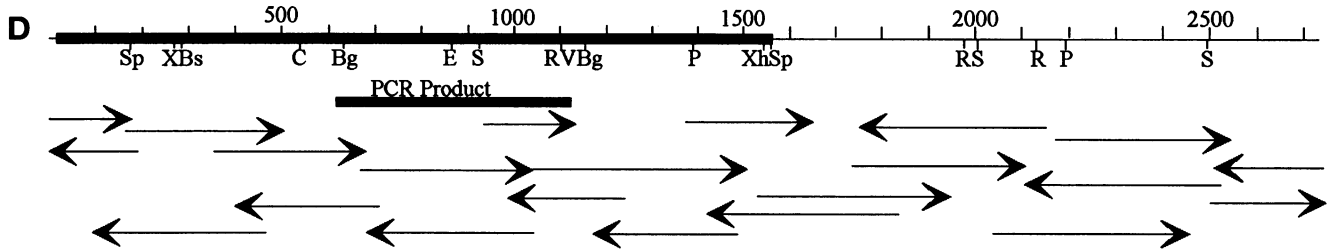
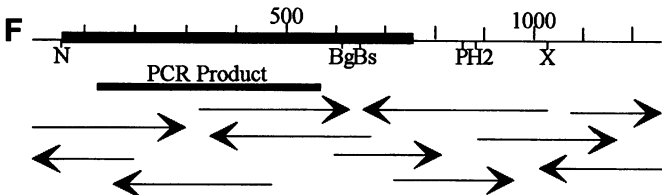


Figure 1.

C CGGGCCAGCACAGATGGCGTTCGACGCGATCGGGGAATCGTGAACGGGGCCGACCCGAACTGCCCGTCCCGATGGCCGGAGCTCGCCACCAGGCGCTGGCGGTGG 120
 M A L R A M R G I V N G A A P E L P V P T R P P M A G A R E Q A L A V (35)
 GCGGGAACACCTATCCCAGCCTCGTCTCACCTACAAGACTGTCTCTGGGTGAATGGTCCACTAGTGATCCTAGATCATCTGAAGTTTCCAGATACGCTGAGATTGCCACTTGACAT 240
 G R N Y L S Q P R L T Y K T V S G V N G P L V I L D H V K F P R Y A E I V H L T (75)
 TACCAGATGGCACAAAGAAAGTGGGGCAAGTCTAGAAGTTAGTGGCTCCAAGCAGTGGTTCAGGATTTGAAGGGACATCTGCTATAGACGCCAAGAAAACATCCCTGTGAGTTTACTG 360
 L P D G T K R S G A S L E V S G S A A V V Q V F E G T E G I V A K K T S C E F T (115)
 GAGATATTCCGAACACCACTGTCTGAGGATATGCTTGGTGGGTATCAACGGATCAGGAAAACCCATTGACCCAGGCGCTGTGGTGTGGTGAAGACTTCCTTGACATCGGGTGC 480
 G D I L R T P V S E D M L G R V F N G S G K P I D R G P V V L A Z D F L D I M G (155)
 AGCCAATCAACCTCAGTGTGGATCTATCCAGAAGAGATGATTACAGCGGGCATTCCGCCATCGATGGCATCAACAGTATTGCTAGGGGACAGAAAATCCCGATCTTTCTGTGTGTG 600
 Q P I N P Q C R I Y P E E M I Q T G I S A T D G M N S I A R G Q K I P I F S A A (195)
 GATTACCCATAACGAGATTGCAGCTCAGATCTGTGCGCCAGGCTGGTTGGTAAAGAAATCAAAGATGTAGTGAGCATATAGTGAAGAAAATTTGCCATTGTGTTTGTCTATGGGAG 720
 G L P H N E I A A Q I C R Q A G L V K K S K D V V D Y S E E N F A I V F A A M G (235)
 TAAACATGGAAACGCCCGGTTCTTTAAATCTGACTTTGAAGAAAATGGCTCAATGGACAATGTCTGCGTGGTTTGTGCTTGGCTAATGACCAACCATTGAGCGGATCATCACTCCCT 840
 V N M Z T A R F F K S D F Z E N G S M D N V C L F L I L P N D P T I Z R I I T P (275)
 GCCTGGCTCTGACCCAGCGAGTTTCTGCGATCATGAGTGTGAGAAGCAGTGTGCTGCTGAGTCTGCTTCCGAAAGCGCTTCGAGAGGTTTTCAGTCCAGGGAAG 960
 C L A L T T A Z F L A Y Q C Z K H V L V I L T D T S S Y P Z A L R E V S A A R E (315)
 AGGTCCCTGGTCCGGAGGCTTCCAGGCTACATGTATACCGACTTAGCCACAATATGAAACGCGCGTGGAGTGGAAAGTAGAAACGGCTCTATTACCCAAATCCCTATTCTCACA 1080
 Z V P G R R Q F P G Y M Y T D L A T I Y Z R A G R V Z G R N G S I T Q P I L T (355)
 TGCCCAATGACGATCATCCATCCCTGACTGACTGGCTACATTAAGGGCCAGATCTATGTGACAGACAGCTGCACAACAGACAGATTACCTCTCTATTAAATGTGCTGC 1200
 M P N D D I T H I P D L T G Y T T Z G I A Y D V D R Q L H N R Q I Y P P I N V L (395)
 CCTCACTCTCGTGTAAAGTCACTATCGGAGAAGGAATGACCAGAAGGATCACGCTGATGTGCTAAACAGTGTATGCGTGTATGCCATCGGTAAGGACGTCGAAGCCATGA 1320
 P S L S R L M K S P I G Z G M T R G D H A D V G N Q L Y A C Y A I G K D V Q A M (435)
 AAGCCGTGGGAGAGGAAGCCGCTGACCTCGGATGATCTGCTTTACCTGGAATTTCTGACAGAATTTGAGAGAATTCATTACTCAGGTCCTATGAAAACCGAAGCTGTTATGAGA 1440
 G A V V G Z Z A L T S D D L L Y L Z F L Q K F Z K N F I T Q G P Y Z N R T V Y Z (475)
 CTTTGGACATGGCTGCTCGAATCTCCCAAGAAATGCTGAAGAGAATCCCTCAGAGCACTTCCAGCAAGTAACTTACCTCAGAGCTCGCAAGCACTAGTAGCTGCTGC 1560
 T L D I G W Q L T R I P P K Z M L K R I P Q S T L S Z F Y P R D S A K H -* (511)
 TGCTTGTGGCGTACCCCTCTGAAGTACTGGTTCTGTTCTCCTGATTCTTTCGACTCCTCCATCCACCTATGAGTGGGAGTTACCTGTACCCCTGTAATTAACAAGGCTA 1680
 GGTAACATTTGGCAGTGTGACAGTTTAAACTGCTAACAGATTGAGAGATCCCTGCTCAGAAACCTCACCTTGTAGTCTCTTTAAAGAAGCTGAGGGTGAAGTTTGTCTACTGATG 1800
 TATCTATTGTACAGATAGTGGAGAGCTAGTTGCTAATAATGTCTTGTGGTCTCCCAAACCTACCTCTCAACTCCCTTAAGAGTATCACTGTTCTGAAGCTAAATGCTTCAGTCT 1920
 CAATTTAGGGGCAAAGTCGAGCCTGGAAGAATCTCTCTTTCAGAAGAACCACGAGGCTCTGGCTGAGTCCCTCTGGAGTGTAGTGTCCCTGTGGTCTGCTCTCGTGCAGA 2040
 TGGTGTACTGTCTGCTTCTTACGAAAAGAGTTCGTTCTGCGAGTGTGAGTGGAAATTCCTGCGTGGCGACTTCTCTGAGGCCACAGAGAATCAGGTAACATTGCA 2160
 CAGCCTCGTCTCTGCTGAGTGTGGCAGCCGCTGCTGACGACCCCACTGGCTACAGTACAGGAGAATTGAGACTTGGAAAAGGCTAGGGTACAATTAAGAAAACCCCTACATCCC 2280
 ACCCTCTCTTGAACCGTCTCTCCCTCTGCGTGTGCGCTCCAGATCTGAGGTGGGGCTGAGAGAGACTTGTCTTAACTGTTAATCCCCAGGCTTTGTGAGTCCGCTCT 2400
 ACCTTTCTGGGATCTTGTGACATGTAGCAATGTTCTTTCATCTCTGCTCCCTCCTGGCTGAGCTCTGGCTGATTTCTGTGTGCTCTACCATGTCTGCTGTTGGTCTCTG 2520
 CGCTGTGTTTCTCAGGTGCGACCATGACTCCCCACTCTGTCATCCACCTCCAGTGTGTTTCTCTGAGGGGATAGTGGGGGGGACGAGGATTATATTTAATGTAGAAAATGTG 2640
 ACATCTCGTTATAAATGAAAATGTTAAATTAATGGA_n 2690



E TTTGCTCCGCGCCACTTTGAACCCAGATTCGAAGCTGTCCCTGGCCGGAATTTGCCCTTTCGCCATGGGCTCAGGCATGACAGATGTACAGAAGCAGATTAAGCACATGATGGCTTCA 120
 M G L R H A D V Q K Q I K H M M A F (18)
 TTGAACAAGAACCAATGAGAAGCAGAAGAAGATATAGATGCAAGGCAGAAGAAGAGTTCACACATGGAGAAAGTTCGCCCTTCGAAAACGAAAGCTGAAGATTATGGAATACTACG 240
 I E Q E A N E K A E E E I D A K A E E E F N I E K G R L L E T Q R L K I M E Y Y (58)
 AGAAGAAGAAAAGCAGATTAGACAGCAGCAGAGAAAATTCAGATGTCCAACTTGTGATCAAGCAAGGCTCAAAGTCTCAGAGCAAGGATGACCTCATCTGATCTACTAATTG 360
 E K K E K Q I R Q Q K K I Q M S N L M N Q A R L K V L R A R D D L I T D L L N (98)
 AGCAAGCAGAGATCATGAAGTGTGAAAAGATACGACCCGTTACCAAGTGTCTGTGATGGCTGGTCTCAGGCTTGTACCAGCTGTGAGCCTCGAATGATCGTGCCTGCA 480
 E A K Q R L M K V V K D T T R Y Q V L L D L G L V L Q G L Y Q L L E F R M I V R C (138)
 GAAAACAAGATTTCCTTTGGTGAAGGCGCAGTACAAAAGCAATCCCTATGTATAAAATTTGTCACAAAAGAGATGTGGATGTGCAAAATCGACCAAGGCTACCTGCTGAGGAACA 600
 R K Q D F P L V K A A V Q K A I P M Y K I A T K R D V D V Q I D Q E P T C L R N (178)
 TAGCTGGTGGCTGTGATCTATAATGGGGATCGCAAGATAAAGTTTCCAACCCCTGAAAAGCGGCTGGACCTGATAGCCAGCAGATGATGCCAGAAGTCCGTGGAGCCTGTGTTG 720
 I A G G V E I Y N G D R K I K V S N T L E S R L D L I A Q Q M M P E V R G A L F (218)
 GTGCAATCCCAATGGAAGTTTCTGACTTAGCTTACAGGAGGAGCAGTTCACCCAGGCTGTTCTCCTGGAGAAGCAGATATCTGTGTGGCTTCTCTTCTGTCTAATACCGGTAATC 840
 G A N A N R K F L D (228)
 AGTGACCTCTGACGTAATGCCCTCGCTCAGTCTCAACAGCAGGGCCACTTGGTGTGGGCAAGAACCCAGCCCGAGCTCATCTGAGGCCACAGCTGTTCACTGGGTTGACGACAGGCG 960
 GGAGCTCAGATGTGCTGCACGGCTCACCCAGGACCAATCTTCCCTGTCTGCTAGTCTAGTGTAGTTGTGCATGCTGCTCCTGCTCTTGGGCATAAAGTGATGTGGGGACT 1080
 CACATTCCTCCAGAACACTACCTTCTGCTTACTCTTTAGTCTAGTCTTCTCTCTGTAATGTGATTTAAATCTAAGCCACAATATTCTTTATTATTAACAGAGGGCTTAT 1200
 GTGGA₂₀ 1294



(Figure 1 cont.) Sequences and restriction maps of the mouse V-ATPase subunit cDNAs. (A) DNA sequence and predicted amino acid sequence for subunit A (70-kDa subunit). (B) An abbreviated restriction map for subunit A. (C) DNA sequence and predicted amino acid sequence for subunit B (60-kDa subunit). (D) An abbreviated restriction map for subunit B. (E) DNA sequence and predicted amino acid sequence for subunit E (31-kDa subunit). (F) An abbreviated restriction map for subunit E.

(A, C, and E) The PCR products are shown by underlining. (B, D, and F) The dark bars superimposed on the lines representing the cDNA indicate the regions of the PCR products, while the open-reading frames, while the dark bars shown below indicate the regions of the PCR products. Shown also are the sequencing strategies followed. Restriction sites indicated are as follows: B, BamHI; Bg, BglII; Bs, BstXI; C, ClaI; E, EagI; H, HindIII; H2, HincII; N, NcoI; P, PstI; RI, EcoRI; RV, EcoRV; S, SacI; Sp, SpeI; X, XbaI; and Xh, XhoI. Accession numbers for these sequences are as follows: (A) U13837; (C) U13838; and (E) U13841.

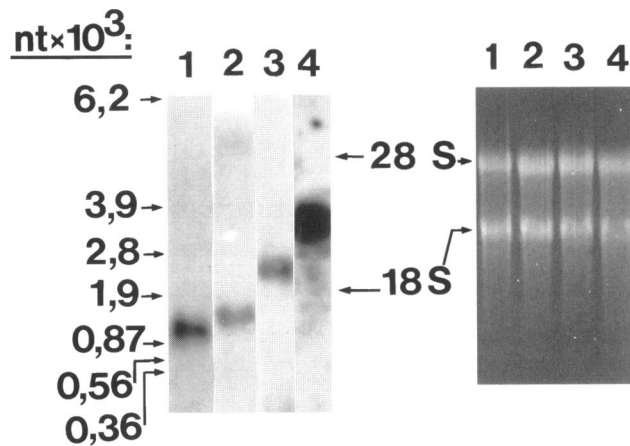


Figure 2. Northern blots from cultured osteoclasts probed with the different V-ATPase subunit cDNAs. Total RNA was separated by formaldehyde agarose gel electrophoresis, transferred to nitrocellulose membrane, and probed with PCR products corresponding to the 16-kDa subunit (1), the 31-kDa subunit (2), the 60-kDa subunit (3), and the 70-kDa subunit (4). Northern blot (left) and total RNA stained with ethidium bromide (right) are shown.

CA II protein and the 16-kDa V-ATPase mRNA

confirmed the polarized distribution of the latter (Figure 3k).

Localization of the mRNAs for the 31-, 60-, and 70-kDa subunits of V-ATPase was also studied in resorbing and nonresorbing osteoclasts, and a similar polarization of mRNAs in the resorbing osteoclasts was observed (Figure 4, b, e, and h). However, when cells were not located on a resorption lacuna, the corresponding mRNAs were diffusely distributed, and found also above the highest nuclei (Figure 4, c, f, and i). It seems that mRNAs for these V-ATPase subunits change their polarization in osteoclasts during the resorption cycle. From these data it was not, however, possible to conclude whether this is due to an actual reorganization of existing transcripts, or whether there is a degradation of the existing transcripts and a rapid, direct targeting of the newly synthesized mRNAs during the polarization process.

Cytoskeleton Involvement

The role of the cytoskeleton in mRNA polarization has also previously been discussed (Cheng and Bjercknes 1989; Sundell and Singer, 1991; Singer, 1992; Rings *et*

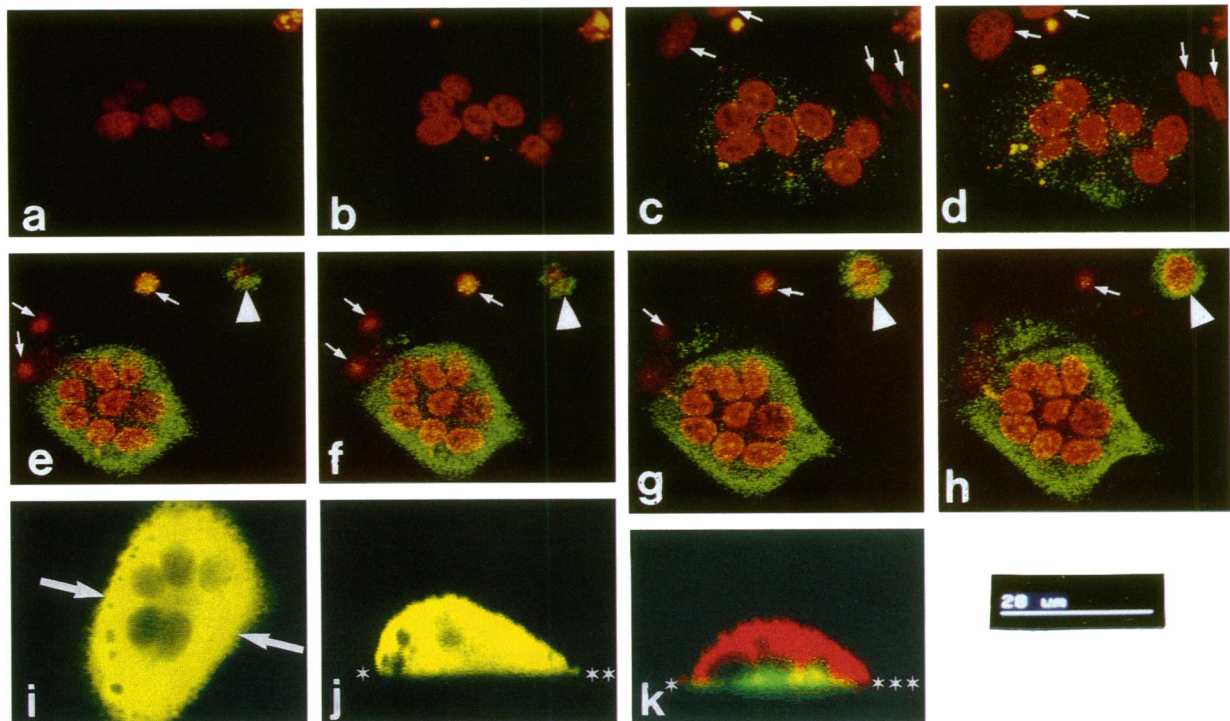


Figure 3. Pseudocolored confocal images of the bone-resorbing osteoclasts cultured on bone slices after in situ hybridization. Nuclei (red) and mRNAs (green) coding for the 16-kDa V-ATPase subunit (a–d) or CA II (e–h) in XY-optical sections from the cell top (a and e) toward the bone surface (d and h) with 3- μ m intervals. Mononuclear cells not expressing mRNA are marked with small arrows (c–h), and a mononuclear cell expressing CA II mRNA is marked with an arrowhead (e–h). Double staining of CA II mRNA (green) and protein (red) in a resorbing osteoclast in the XY-plane (i) and the XZ-plane (j). The site of the the XZ-slice is shown with arrows in panel i. The color becomes yellow when the stainings overlap. Double staining of the 16-kDa V-ATPase subunit mRNA (green) and CA II protein (red) in a resorbing osteoclast in the XZ-plane (k). Bone surface is marked with asterisks in panels j and k. Bar, 20 μ m.

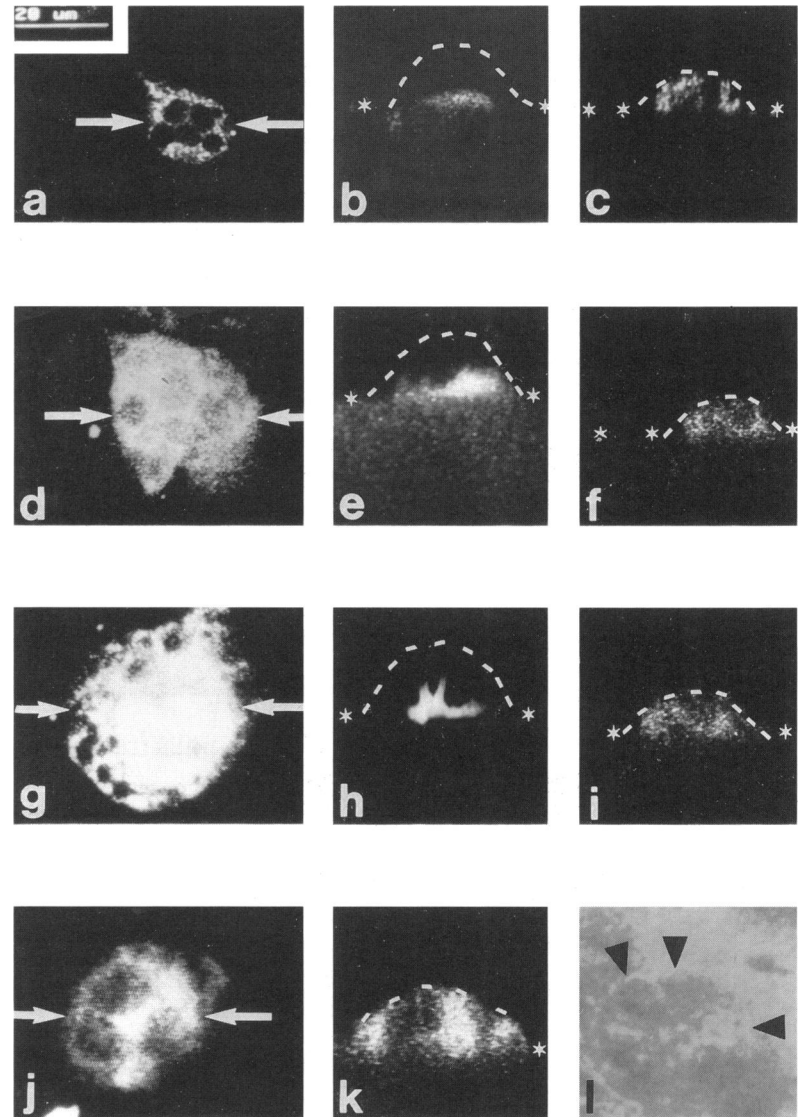


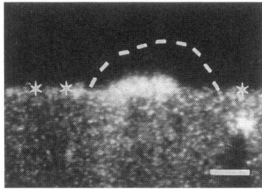
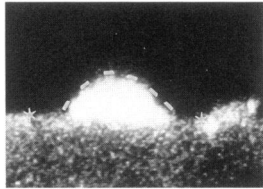
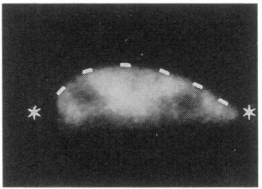
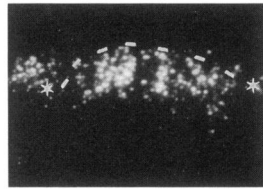
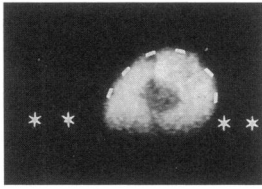
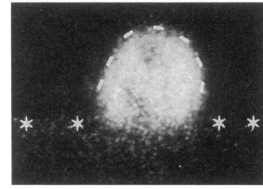
Figure 4. Confocal images of the in situ localization of mRNAs coding for the V-ATPase subunits of 31 kDa (a–c), 60 kDa (d–f), and 70 kDa (g–i), or γ -actin (j–l). Resorbing osteoclasts in the XY-plane (a, d, g, and j), where the site of the XZ-slice is shown with arrows. In the corresponding XZ-plane (b, e, h, and k), the top of the highest nuclei is marked with a broken line and bone surface is marked with asterisks. Nonresorbing osteoclasts in the XZ-plane (c, f, and i), where the cell top is marked with a broken line and bone surface is marked with asterisks. The resorption lacuna excavated by the osteoclast in panels j and k is marked with arrowheads in panel l. Bar, 20 μ m.

al., 1994). To study this question, we exposed resorbing osteoclasts to colchisin, cytochalasin B, or dbcAMP, all of which we thought might have an influence on the polarization of osteoclasts. For dbcAMP, specific effects on osteoclast microfilaments have previously been described (Lakkakorpi and Väänänen, 1990), and colchisin and cytochalasin B are known to effect microtubule and actin fiber growth. As can be seen from Table 1, colchisin had no effect on mRNA polarization. Cytochalasin B caused a decrease in mRNA levels, and inhibited mRNA polarization. We found that dbcAMP that disperses the actin ring in resorbing osteoclasts, had a distinct effect on the polarization of the 16-kDa V-ATPase mRNA; polarization of the 16-kDa V-ATPase mRNA was lost, and the amount of transcript was much higher than in the nonresorbing control cells. The effects of colchisin,

cytochalasin B, and dbcAMP on the morphology of actin fibers and microtubules are shown in Table 2. As expected, dbcAMP dispersed all actin ring structures within 20 min, but had no effect on microtubules. Similar effects were also seen after treatment with cytochalasin B. Disruption of actin fibers with cytochalasin B was, however, slower than with dbcAMP. Colchisin disrupted microtubules specifically within 20 min, and when applied for 24 h was toxic to multinuclear cells.

Bafilomycin A₁, a specific V-ATPase inhibitor (Hanada *et al.*, 1990; Sundquist *et al.*, 1990; Mattsson *et al.*, 1991) also inhibited polarization of the 16-kDa V-ATPase mRNA. On the basis of our in situ hybridization experiments, synthesis of the 16-kDa subunit mRNA seemed to be highly stimulated, but the transcripts showed no polarization (Figure 5b). This effect seemed

Table 1. Effects of colchisin, cytochalasin B, and dbcAMP on mRNA polarization in cultured osteoclasts.

DRUG	LOCALIZATION OF	
	16 kD mRNA	CA II mRNA
25 μ M Colchisin	 normal	 normal
20 μ M Cytochalasin B	 polarization disappears	 normal
1 mM dbcAMP	 polarization disappears	 normal

Top of the highest nuclei is marked with a broken line, and bone surface with asterisks. Confocal images are taken in the XZ-plane. Bar, 10 μ m; n = 250.

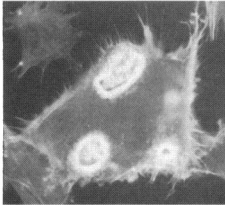
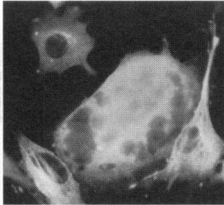
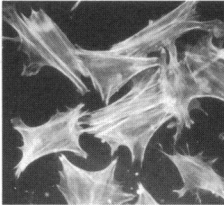
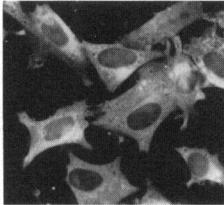
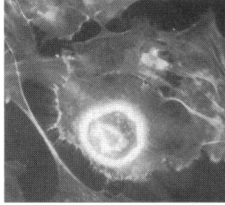

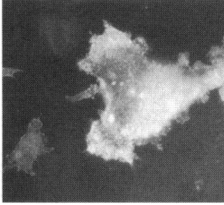
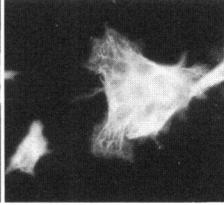
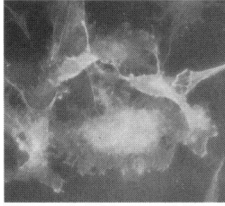
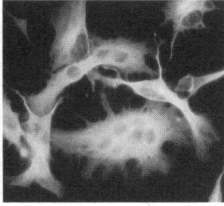
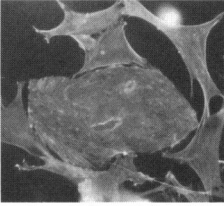
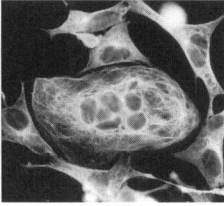
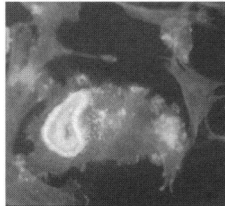

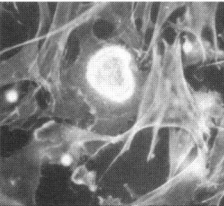
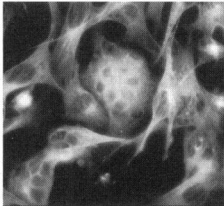
to be dose dependent (Figure 5). To confirm this, Northern blots were made from cultured cells treated with different bafilomycin A₁ concentrations. These results showed that the amount of 16-kDa V-ATPase mRNA was increased with bafilomycin A₁ (Figure 6).

Antisense Effects

To study further the localization of V-ATPase mRNA in osteoclast polarization, antisense RNA transcripts corresponding to the previously used cDNA fragments targeted against the 16-kDa or 60-kDa V-ATPase subunits or against CA II were added to rat osteoclast cultures. As a hallmark for polarization and

activity of osteoclasts, the specific arrangement of F-actin in resorbing osteoclasts was used. Antisense RNAs for the 16-kDa and 60-kDa V-ATPase subunits decreased specifically the number of actin rings in osteoclasts, suggesting disturbance of polarization of the osteoclasts, whereas CA II antisense RNA had no effect on the number of actin rings, leaving the osteoclast polarization unchanged (Figure 7 and Table 3). In spite of this difference between V-ATPase and CA II antisense effects upon polarization, they both inhibited bone resorption to about the same extent (Table 3). Thus, it seems that normal expression of V-ATPase is required for proper polarization of the osteoclasts,

Table 2. Effects of colchisin, cytochalasin B, and dbcAMP on the morphology of actin fibers and microtubules (MT) in osteoclast cultures.

DRUG	After 20 min		After 24 h	
	Actin	MT	Actin	MT
25 μ M Colchisin				
20 μ M Cytochalasin				
1 mM dbcAMP				
Vehicle				

Drugs were added to the cultures in the beginning of the culture (24 h) or after a 24h preculture (20 min). Cells were then fixed and stained with phalloidine and a monoclonal anti α -tubulin antibody.

whereas CA II expression, although obligatory for resorption itself, is not critical for osteoclast polarization. We have previously shown by immunostaining and immunoprecipitation that CA II antisense DNA and RNA decrease CA II protein expression (Laitala and Väänänen, 1994). A clear decrease in the amount of CA II and 60-kDa V-ATPase subunit protein was seen after antisense RNA treatment. The antisense RNAs were also able to decrease the amount of specific mRNA in the osteoclast cultures, as seen after Northern blotting (Figure 8). These results were further confirmed by Western blotting using antibodies against CA II and the 60-kDa subunit of V-ATPase (Figure 9). We were not able to obtain antibodies

against the 16-kDa subunit of V-ATPase, so no immunological experiments with this subunit were possible. However, we have previously shown a decrease in RNA-levels for CA II and the 16-kDa V-ATPase subunit after antisense treatment using quantitative PCR (Laitala and Väänänen, 1994).

DISCUSSION

We have studied the localization of the 16-, 31-, 60-, and 70-kDa V-ATPase subunit mRNAs in osteoclasts during the resorption cycle, and noticed a clear polar distribution of these mRNAs in resorbing osteoclasts. The mechanism resulting in polar-

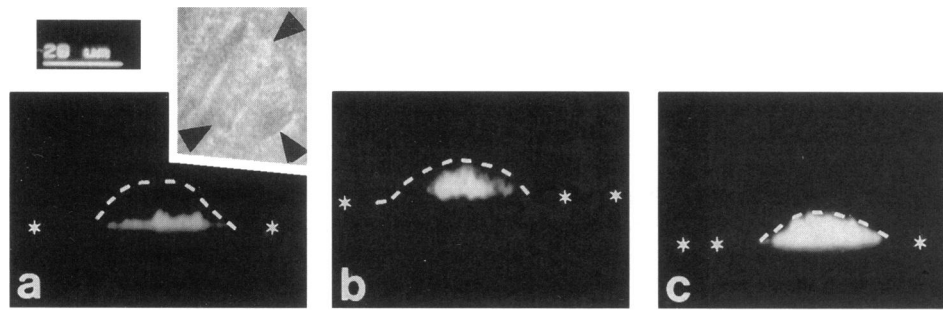


Figure 5. Confocal images of the effects of bafilomycin A₁ on the expression of mRNA for the 16-kDa V-ATPase subunit. Control osteoclast in the XZ-plane (a), and the corresponding lacuna (XY-plane), which is marked with arrowheads. Osteoclasts treated with 1 nM (b) or 10 nM (c) bafilomycin A₁ in the XZ-plane. The top of the highest nuclei is marked with a broken line, and bone surface is marked with asterisks in all figures. Bar, 20 μm.

ization of these mRNAs in cultured osteoclast is unknown, but two possibilities may be considered. The polarization we have observed may be the result of polarized secretion of mRNA from the nuclei or may result from specific post-transcriptional sorting of existing mRNAs already present in the cytoplasm. Direct signal-sequence-derived sorting of mRNA has been reported for membrane proteins and secreted proteins (Yisraeli and Melton, 1988; Sundell and Singer, 1990; Wang *et al.*, 1991). In cultured fibroblasts, specific spatial distribution of three cytoplasmic protein mRNAs can be seen: actin mRNA is found in lamellipodia, vimentin mRNA is found in the perinuclear region, and tubulin mRNA is found in the peripheral cytoplasm (Lawrence and Singer, 1986; Singer *et al.*, 1989). In the brain, MAP2 mRNA is only located in the dendrites but not the cell body (Garner *et al.*, 1988). This polarization seems also to have a physiological relevance, because the majority of MAP2 protein is located in the dendrites. A specific dendritic targeting signal for MAP2 has thus been suggested (Papandrikopoulou *et al.*, 1989). In resorbing osteoclasts a major part of V-ATPase is located at the ruffled border membrane pumping protons into the resorption lacuna (Blair *et al.*, 1989; Väänänen *et al.*, 1990). Thus, the polariza-

tion of mRNA seems to precede the polarized distribution of the final gene product.

It has been shown that mRNA may contain sorting information in the 3'-noncoding region (Macdonald and Struhl, 1988; Yisraeli and Melton 1988). It has also been suggested that the 3'-noncoding signal could

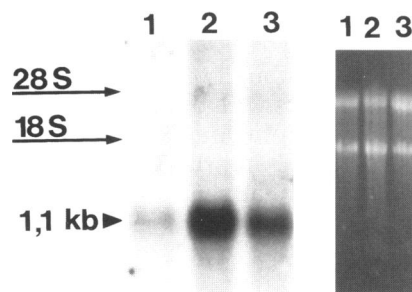


Figure 6. Northern blotting from osteoclast cultures treated with different concentrations of bafilomycin A₁. Control (lane 1), 1 nM bafilomycin A₁ (lane 2), and 10 nM bafilomycin A₁ (lane 3). Northern blot is shown on the left and total RNA stained with ethidium bromide is shown on the right.

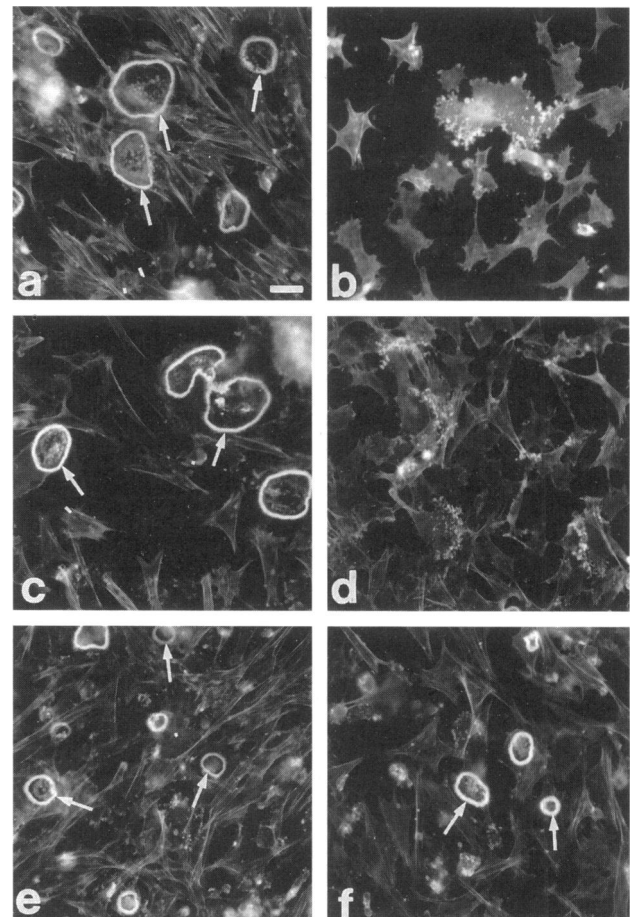


Figure 7. Morphology of actin rings after antisense treatment as follows: the 16-kDa sense RNA (a); the 16-kDa antisense RNA (b); the 60-kDa sense RNA (c); the 60-kDa antisense RNA (d); CA II antisense RNA (e); and 1 nM bafilomycin A₁ (f). Arrows point to the actin rings in osteoclasts. Bar, 20 μm in a–d, and 40 μm in e and f.

Table 3. Number of actin rings in osteoclast cultures after antisense treatment

Sample	Number of osteoclasts/ bone slice \pm SD	Number of actin rings/ bone slice \pm SD	Resorbed area, μm^2 / osteoclast \pm SD
Control	260 \pm 21	140 \pm 17	968 \pm 145
16-kDa antisense RNA	271 \pm 24	58 \pm 10 (***)	632 \pm 89.1
16-kDa sense RNA	253 \pm 19	129 \pm 16	1031 \pm 129
60-kDa antisense RNA	269 \pm 17	63 \pm 8 (***)	593 \pm 92.9
60-kDa sense RNA	252 \pm 12	147 \pm 25	899 \pm 102
CA II antisense RNA	271 \pm 17	121 \pm 21	721 \pm 118
CA II sense RNA	239 \pm 15	144 \pm 29	1106 \pm 138

Osteoclasts were counted after Hoechst staining and actin rings after phalloidin staining. Resorbed area was measured after WGA-lectin staining of bone slices (***, $p < 0.001$). $n = 6$.

interact directly or via a carrier protein with the cytoskeleton. This would lead to mRNA sorting into specific sites in the cytoplasm, and translation inside these compartments (Rings *et al.*, 1994). The 16-kDa V-ATPase subunit is a hydrophobic membrane protein that might be polarized at the mRNA level according to its signal sequence. Although translation of this protein is normally thought to occur simultaneously with translocation into the endoplasmic reticulum, it may be that translation at the ruffled border site leads to the incorporation of the hydrophobic protein directly into the ruffled border membrane. The hydrophilic subunits may be sorted in a similar manner or with the help of the cytoskeleton. The osteoclast cytoskeleton undergoes a tremendous reorganization during the resorption cycle. The significance of the cytoskeleton may, in addition to the polarization, extend to mRNA sorting, as described earlier for other mRNA molecules (Bonneau *et al.*, 1985; Ornelles *et al.*, 1986; Macdonald and Struhl, 1988; Sundell and Singer, 1991). Cytoskeletal changes would also explain why the V-ATPase subunit mRNAs are diffusely distributed in nonresorbing osteoclasts.

Bafilomycin A₁, which inhibits bone resorption at nanomolar concentrations, seems to increase the transcription of the 16-kDa V-ATPase subunit. We currently have no explanation for this phenomenon, but it suggests the existence of a feedback mechanism that would provide for the production of more mRNA for the 16-kDa V-ATPase subunit, when the function of the V-ATPase is blocked. It would be of interest to find out whether polarized targeting of mRNA is directly dependent on acidification of some intracellular compartments or vesicular traffic, or whether the effect of bafilomycin A₁ is indirect. However, mRNA for CA II, which is a soluble protein, seems to be localized normally even in the presence of bafilomycin A₁.

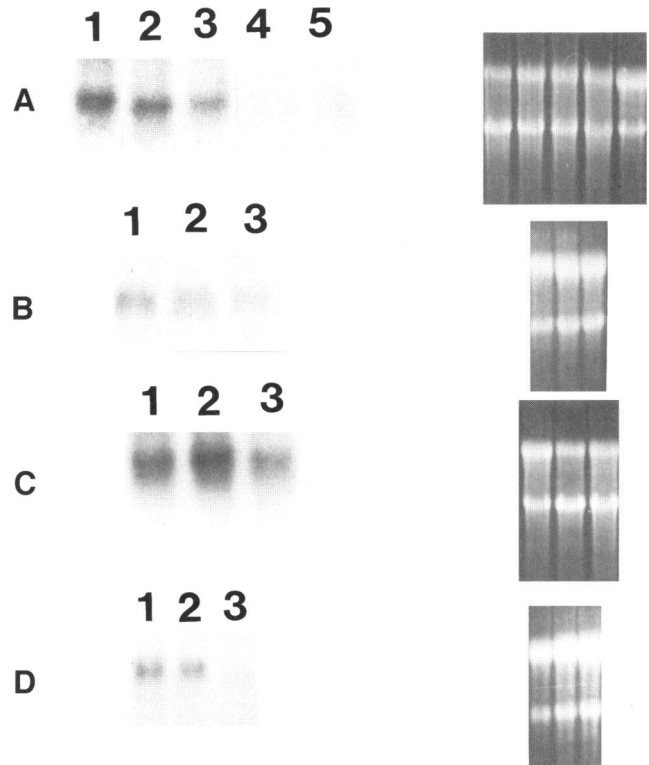


Figure 8. Northern blotting (left) from osteoclasts cultured in the presence of antisense RNA. Total RNAs stained with ethidium bromide are shown on the right. (A) The 16-kDa V-ATPase subunit probe localization in control (lane 1) and samples treated with scrambled RNA (lane 2), sense RNA (lane 3), antisense RNA (lane 4), or antisense DNA (lane 5). (B) The 60-kDa V-ATPase subunit probe localization in control (lane 1) and samples treated with sense RNA (lane 2) or antisense RNA (lane 3). (C) The 70-kDa V-ATPase subunit probe localization in control (lane 1) and samples treated with sense RNA (lane 2) or antisense RNA (lane 3). (D) CA II probe localization in control (lane 1) and samples treated with sense RNA (lane 2) or antisense RNA (lane 3).

Previous studies have shown that yeast mutants lacking the 16-kDa or 100-kDa V-ATPase subunits (V₀ complex) cannot assemble the other cytoplasmic subunits (V₁ complex) onto the vacuole (Umamoto *et al.*, 1990; Noumi *et al.*, 1991; Kane *et al.*, 1992), whereas the V₁ complex is not needed for the V₀ complex to be targeted to the yeast vacuole. Other studies have addressed the necessity of individual subunits in the formation of the V₁ complex (Kane, 1992; Doherty and Kane, 1993; Ho *et al.*, 1993). The 27-kDa, 60-kDa, and 70-kDa subunits seem to be vital for this event, whereas lack of the 42-kDa subunit does not block V₁ complex formation. These results suggest that key subunits of the V-ATPase must be present for the enzyme complex to be functional. This can also be seen in our antisense experiments, where bone resorption is decreased, when specific subunits are not present in the V-ATPase. On the other hand, mRNA

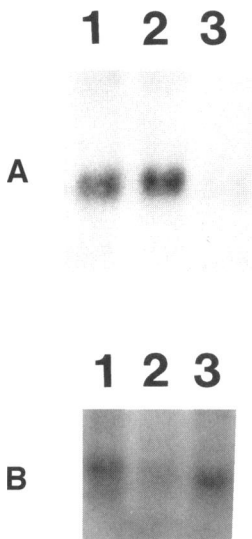


Figure 9. Western blotting from osteoclasts cultured in the presence of antisense RNA. (A) CA II antibody staining in control (lane 1) and samples treated with sense RNA (lane 2) or antisense RNA (lane 3). (B) The 60-kDa V-ATPase subunit antibody staining in control (lane 1) and samples treated with antisense RNA (lane 2) or sense RNA (lane 3).

synthesis itself is vital for bone resorption (Hall *et al.*, 1993). Cell-specific V-ATPase subunit sequences have been previously suggested (Nelson *et al.*, 1992; Nezu *et al.*, 1992; Puopolo *et al.*, 1992), but only recently has the first evidence for the existence of specific isoforms of V-ATPase subunits in human osteoclastoma appeared (Chatterjee *et al.*, 1992; van Hille *et al.*, 1993a,b, 1994).

Antibodies and cDNA probes were used to study the specificity of the antisense RNA molecules on translation inhibition. The results obtained were in agreement with our previous data showing no non-specific side effects. The antisense RNAs were able to decrease both the amount of mRNA and protein. This data suggests that the antisense RNAs were able to inhibit translation, and possibly increase the disposal of the specific mRNA. Antisense mRNA targeted against V-ATPase subunit A has been successfully used to inhibit V-ATPase in carrot (Gogarten *et al.*, 1992).

Our results clearly show that the distribution of mRNAs for several V-ATPase subunits in osteoclasts is dependent on the polarity of the cell. Our antisense experiments further suggest that expression of these proteins located in the ruffled border membrane is also crucial for polarization itself. Changes in the distribution of RNA transcripts during the resorption cycle in osteoclasts indicate that at least large, multinucleated cells must have specific and dynamic mechanism(s) for mRNA targeting and translocation.

ACKNOWLEDGMENTS

We thank Allan Haimakainen, Xu Jin, Eero Oja, and Minna Orveteläinen for technical assistance and Dr. Tom Stevens for the *vat2* deletion strain. This study was supported by the Sigrid Juselius Foundation, the Finnish Academy of Sciences, National Institutes of Health grant GM-39555 (G.E.D.), and American Heart Association Fellowship AHA SW-92-27 (M.L.H.).

REFERENCES

- Ausubel, F.M., Brent, R., Kingston, R.E., Moore, D.D., Seidman, J.G., Smith, J.A., and Struhl, K. (1992). *Current Protocols in Molecular Biology*, New York: John Wiley & Sons.
- Berleth, T., Burri, M., Thoma, G., Bopp, D., Richstein, S., Frigerio, G., Noll, M., and Nusslein-Volhard, C. (1988). The role of localization of *bicoid* RNA in organizing the anterior pattern of the *Drosophila* embryo. *EMBO J.* 7, 1749–1756.
- Blair, H.C., Teitelbaum, S.L., Ghiselli, R., and Gluck, S. (1989). Osteoclastic bone resorption by a polarized vacuolar proton pump. *Science* 245, 855–857.
- Bonneau, A.-M., Darveau, A., and Sonenberg, N. (1985). Effect of viral infection on host protein synthesis and mRNA association with the cytoplasmic cytoskeletal structure. *J. Cell Biol.* 100, 1209–1218.
- Bowman, B.J., Allen, R., Wechsler, M.A., and Bowman, E.J. (1988a). Isolation of genes encoding the *Neurospora* vacuolar ATPase. *J. Biol. Chem.* 263, 14002–14007.
- Bowman, E.J., Tenney, K., and Bowman, B.J. (1988b). Isolation of genes encoding the *Neurospora* vacuolar ATPase: analysis of *vma-1* encoding the 67-kD subunit reveals homology to other ATPases. *J. Biol. Chem.* 263, 13994–14001.
- Chatterjee, D., Chakraborty, M., Leit, M., Neff, L., Jamsa-Kellokumpu, S., Fuchs, R., and Baron, R. (1992). Sensitivity to vanadate and isoforms of subunits A and B distinguish the osteoclast proton pump from other vacuolar H⁺-ATPases. *Proc. Natl. Acad. Sci. USA* 89, 6257–6261.
- Cheng, H., and Bjerknes, M. (1989). Asymmetric distribution of actin mRNA and cytoskeletal pattern generation in polarized epithelial cells. *J. Mol. Biol.* 210, 541–549.
- Curtis, P.J., Withers, E., Demuth, D., Watt, R., Venta, P.J., and Tashian, R.E. (1983). The nucleotide sequence and derived amino acid sequence of cDNA coding for mouse carbonic anhydrase II. *Gene* 25, 325–332.
- Doherty, R.D., and Kane, P.M. (1993). Partial assembly of the yeast vacuolar H⁺-ATPase in mutants lacking one subunit of the enzyme. *J. Biol. Chem.* 268, 16845–16851.
- Foury, F. (1990). The 31-kD polypeptide is an essential subunit of the vacuolar ATPase in *Saccharomyces cerevisiae*. *J. Biol. Chem.* 265, 18554–18575.
- Garner, C.C., Tucker, R.P., and Matus, A. (1988). Selective localization of messenger RNA for cytoskeletal protein MAP2 in dendrites. *Nature* 336, 674–677.
- Gay, G.V., and Mueller, W.J. (1974). Carbonic anhydrase and osteoclasts: localization by labeled inhibitor autoradiography. *Science* 183, 432–434.
- Gogarten, J.P., Fichmann, J., Braun, Y., Morgan, L., Styles, P., Taiz, S.L., DeLapp, K., and Taiz, L. (1992). The use of an antisense mRNA to inhibit the tonoplast H⁺-ATPase in carrot. *Plant Cell* 4, 851–864.
- Gu, H.H., Xu, J., Gallagher, M., and Dean, G.E. (1993). Peptide splicing in the vacuolar ATPase subunit A from *Candida tropicalis*. *J. Biol. Chem.* 268, 7372–7381.
- Hall, G.E., and Kenny, A.D. (1987). Role of carbonic anhydrase in bone resorption: effect of acetazolamide on basal and parathyroid hormone-induced bone metabolism. *Calcif. Tissue Int.* 40, 212–218.
- Hall, T.J., Schaeublin, M., and Chambers, T.J. (1992). Na⁺/H⁺-antiporter activity is essential for the induction, but not the maintenance of osteoclastic bone resorption and cytoplasmic spreading. *Biochem. Biophys. Res. Commun.* 188, 1097–1103.
- Hanada, H., Hasebe, M., Moriyama, Y., Maeda, M., and Futai, M. (1991). Molecular cloning of cDNA encoding the 16-kD subunit of

- vacuolar H⁺-ATPase from mouse cerebellum. *Biochem. Biophys. Res. Commun.* 176, 1062–1067.
- Hanada, H., Moriyama, Y., Maeda, M., and Futai, M. (1990). Kinetic studies of chromaffin granule H⁺-ATPase and effects of bafilomycin A1. *Biochem. Biophys. Res. Commun.* 170, 873–878.
- Hesketh, J.E., and Pryme, I.F. (1991). Interaction between mRNA, ribosomes and the cytoskeleton. *Biochem. J.* 277, 1–10.
- Hirata, R., Ohsumi, Y., Nakano, A., Kawasaki, H., Suzuki, K., and Anraku, Y. (1990). Molecular structure of a gene, *VMA1*, encoding the catalytic subunit of H⁺-translocating adenosine triphosphatase from vacuolar membranes of *Saccharomyces cerevisiae*. *J. Biol. Chem.* 265, 6726–6733.
- Hirsch, S., Strauss, A., Masood, K., Lee, S., Sukhatme, V., and Gluck, S. (1988). Isolation and sequence of a cDNA clone encoding the 31-kD subunit of bovine kidney vacuolar H⁺-ATPase. *Proc. Natl. Acad. Sci. USA* 85, 3004–3008.
- Ho, M.N., Hirata, R., Umemoto, N., Ohya, Y., Takatsuki, A., Stevens, T.H., and Anraku, Y. (1993). *VMA13* encodes a 54-kD vacuolar H⁺-ATPase subunit required for activity but not assembly of the enzyme complex in *Saccharomyces cerevisiae*. *J. Biol. Chem.* 268, 18286–18292.
- Hoock, T.C., Newcomb, P.M., and Herman, I.M. (1991). β -Actin and its mRNA are localized at the plasma membrane and the regions of moving cytoplasm during the cellular response to injury. *J. Cell Biol.* 112, 653–664.
- Jackson, R.J. (1993). Cytoplasmic regulation of mRNA function: the importance of the 3'-untranslated region. *Cell* 74, 9–14.
- Jackson, R.J., and Standart, N. (1990). Do the poly(A) tail and 3'-untranslated region control mRNA translation? *Cell* 62, 15–24.
- Kane, P.M., Kuehn, M.C., Howard-Stevenson, I.H., and Stevens, T.H. (1992). Assembly and targeting of peripheral and integral membrane subunits of the yeast vacuolar H⁺-ATPase. *J. Biol. Chem.* 267, 447–454.
- Laitala, T., and Väänänen, K. (1993). Proton channel part of vacuolar H⁺-ATPase and carbonic anhydrase II expression is stimulated in resorbing osteoclasts. *J. Bone Miner. Res.* 8, 119–126.
- Laitala, T., and Väänänen, H.K. (1994). Inhibition of bone resorption in vitro by antisense RNA and DNA molecules targeted against carbonic anhydrase II or two subunits of vacuolar H⁺-ATPase. *J. Clin. Invest.* 93, 2311–2318.
- Lakkakorpi, P.T., Tuukkanen, J., Hentunen, T., Järvelin, K., and Väänänen, K. (1989). Organization of osteoclast microfilaments during the attachment to bone surface in vitro. *J. Bone Miner. Res.* 4, 817–825.
- Lakkakorpi, P.T., and Väänänen, H.K. (1990). Calcitonin, prostaglandin E₂ and dibutylryl cyclic adenosine 3',5'-monophosphate disperse the specific microfilament structure in resorbing osteoclasts. *J. Histochem. Cytochem.* 38, 1487–1493.
- Lakkakorpi, P.T., and Väänänen, H.K. (1991). Kinetics of the osteoclast cytoskeleton during the resorption cycle in vitro. *J. Bone Miner. Res.* 6, 817–826.
- Lawrence, J.B., and Singer, R.H. (1986). Intracellular localization of messenger RNAs for cytoskeletal proteins. *Cell* 45, 407–415.
- Lawrence, J.B., Singer, R.H., Villnave, C.A., Stein, J.L., and Stein, G.S. (1988). Intracellular distribution of histone mRNAs in human fibroblasts studied by in situ hybridization. *Proc. Natl. Acad. Sci. USA* 85, 463–467.
- Macdonald, P.M., and Struhl, G. (1988). *cis*-Acting sequences responsible for anterior localization of *bicoid* mRNA in *Drosophila* embryos. *Nature* 336, 595–598.
- Mandel, M., Moriyama, Y., Hulmes, J.D., Pan, Y.-C.E., Nelson, H., and Nelson, N. (1988). cDNA sequence encoding the 16-kD proteolipid of chromaffin granules implies gene duplication in the evolution of H⁺-ATPases. *Proc. Natl. Acad. Sci. USA* 85, 5521–5524.
- Manolson, M.F., Ouellette, B.F.F., Fillion, M., and Poole, R.J. (1988). cDNA sequence and homologies of the "57-kD" nucleotide-binding subunit of the vacuolar ATPase from *Arabidopsis*. *J. Biol. Chem.* 263, 17987–17994.
- Mattsson, J.P., Väänänen, K., Wallmark, B., and Lorentzon, P. (1991). Omeprazole and bafilomycin, two proton pump inhibitors: differentiation of their effects on gastric, kidney and bone H⁺-translocating ATPases. *Biochim. Biophys. Acta* 1065, 261–268.
- Nelson, H., Madiyan, S., and Nelson, N. (1989). A conserved gene encoding the 57-kD subunit of the yeast vacuolar H⁺-ATPase. *J. Biol. Chem.* 264, 1775–1778.
- Nelson, H., Madiyan, S., and Nelson, N. (1994). A bovine cDNA and a yeast gene (*VMA8*) encoding the subunit D of the vacuolar H⁺-ATPase. *Proc. Natl. Acad. Sci. USA* 92, 497–501.
- Nelson, N. (1989). Structure, molecular genetics and evolution of vacuolar H⁺-ATPases. *J. Bioenerg. Biomembr.* 21, 553–571.
- Nelson, R.D., Guo, X.-L., Masood, K., Brown, D., Kalkbrenner, M., and Gluck, S. (1992). Selectively amplified expression of an isoform of the vacuolar H⁺-ATPase 56-kilodalton subunit in renal intercalated cells. *Proc. Natl. Acad. Sci. USA* 89, 3541–3545.
- Nezu, J., Motojima, K., Tamura, H., and Ohkuma, S. (1992). Molecular cloning of a rat liver cDNA encoding the 16-kD subunit of vacuolar H⁺-ATPases: organellar and tissue distribution of 16-kD proteolipids. *J. Biochem.* 112, 212–219.
- Noumi, T., Beltran, C., Nelson, H., and Nelson, N. (1991). Mutational analysis of yeast vacuolar H⁺-ATPase. *Proc. Natl. Acad. Sci. USA* 88, 1938–1942.
- Ornelles, D.A., Fey, E.G., and Penman, S. (1986). Cytochalasin releases mRNA from the cytoskeletal framework and inhibits protein synthesis. *Mol. Cell. Biol.* 6, 1650–1662.
- Pan, Y.-X., Gu, H.H., Xu, J., and Dean, G.E. (1993). *Saccharomyces cerevisiae* expression of exogenous vacuolar ATPase subunits B. *Biochim. Biophys. Acta* 1151, 175–185.
- Pan, Y.-X., Xu, J., Strasser, J.E., Howell, M., and Dean, G.E. (1991). Structure and expression of subunit A from the bovine chromaffin cell vacuolar ATPase. *FEBS Lett.* 293, 89–92.
- Papandrikopoulou, A., Doll, T., Tucker, R.P., Garner, C.C., and Matus, A. (1989). Embryonic MAP2 lacks the cross-linking sidearm sequences and dendritic targeting signal of adult MAP2. *Nature* 340, 650–652.
- Puopolo, K., Kumamoto, C., Adachi, I., and Forgac, M. (1991). A single gene encodes the catalytic A subunit of the bovine vacuolar H⁺-ATPase. *J. Biol. Chem.* 266, 24564–24572.
- Puopolo, K., Kumamoto, C., Adachi, I., Magner, R., and Forgac, M. (1992). Differential expression of the "B" subunit of the vacuolar H⁺-ATPase in bovine tissues. *J. Biol. Chem.* 267, 3696–3706.
- Rings, E.H.H.M., Buller, H.A., Neele, A.M., and Dekker, J. (1994). Protein sorting versus messenger RNA sorting? *Eur. J. Cell Biol.* 63, 161–171.
- Sambrook, J., Fritsch, E.F., and Maniatis, T. (1989). *Molecular Cloning: A Laboratory Manual*, Cold Spring Harbor, NY: Cold Spring Harbor Laboratory Press.
- Selander, K., Lehenkari, P., and Väänänen, H.K. (1994). The effects of bisphosphonates on the resorption cycle of isolated osteoclasts. *Calcif. Tissue Int.* 55, 368–375.
- Shih, C.-K., Wagner, R., Feinstein, S., Kanik-Ennulat, C., and Neff, N. (1988). A dominant trifluoperazine resistance gene from *Saccha-*

- Saccharomyces cerevisiae* has homology with F_0F_1 ATP synthase and confers calcium-sensitive growth. *Mol. Cell Biol.* 8, 3094–3103.
- Singer, R.H. (1992). The cytoskeleton and mRNA localization. *Curr. Opin. Cell Biol.* 4, 15–19.
- Singer, R.H., Langevin, G.L., and Lawrence, J.B. (1989). Ultrastructural visualization of cytoskeletal mRNAs and their associated proteins using double-label in situ hybridization. *J. Cell Biol.* 108, 2343–2353.
- Sundell, C.L., and Singer, R.H. (1990). Actin mRNA localizes in the absence of protein synthesis. *J. Cell Biol.* 111, 2397–2403.
- Sundell, C.L., and Singer, R.H. (1991). Requirement of microfilaments in sorting of actin messenger RNA. *Science* 253, 1275–1277.
- Sundquist, K., Lakkakorpi, P., Wallmark, B., and Väänänen, K. (1990). Inhibition of osteoclast proton transport by bafilomycin A_1 abolishes bone resorption. *Biochem. Biophys. Res. Commun.* 168, 309–313.
- Sundquist, K.T., Leppilampi, M., Järvelin, K., Kumpulainen, T., and Väänänen, H.K. (1987). Carbonic anhydrase isoenzymes in isolated rat peripheral monocytes, tissue macrophages, and osteoclasts. *Bone* 8, 33–38.
- Trapp, B.D., Moench, T., Pulley, M., Barbosa, E., Tennekoon, G., and Griffin, J. (1987). Spatial segregation of mRNA encoding myelin-specific proteins. *Proc. Natl. Acad. Sci. USA* 84, 7773–7777.
- Umemoto, N., Yoshihisa, T., Hirata, R., and Anraku, Y. (1990). Roles of the *VMA3* gene product, subunit c of the vacuolar membrane H^+ -ATPase on vacuolar acidification and protein transport. *J. Biol. Chem.* 265, 18447–18453.
- Väänänen, H.K., Karhukorpi, E.K., Sundquist, K., Wallmark, B., Roininen, I., Hentunen, T., Tuukkanen, J., and Lakkakorpi, P. (1990). Evidence for the presence of a proton pump of the vacuolar H^+ -ATPase type in the ruffled borders of osteoclasts. *J. Cell Biol.* 111, 1305–1311.
- van Hille, B., Richener, H., Evans, D.B., Green, J.R., and Bilbe, G. (1993a). Identification of two subunit A isoforms of the vacuolar H^+ -ATPase in human osteoclastoma. *J. Biol. Chem.* 268, 7075–7080.
- van Hille, B., Vanek, M., Richener, H., Green, J.R., and Bilbe, G. (1993b). Cloning and tissue distribution of subunits C, D and E of the human vacuolar H^+ -ATPase. *Biochem. Biophys. Res. Commun.* 197, 15–21.
- van Hille, B., Richener, H., Schmid, P., Puettner, I., Green, J.R., and Bilbe, G. (1994). Heterogeneity of vacuolar H^+ -ATPase: differential expression of two human subunit B isoforms. *Biochem. J.* 303, 191–198.
- Wang, A., Cohen, D.S., Palmer, E., and Sheppard, D. (1991). Polarized regulation of fibronectin secretion and alternative splicing by transforming growth factor β . *J. Biol. Chem.* 266, 15598–15601.
- Yisraeli, J.K., and Melton, D.A. (1988). The maternal mRNA *Vg1* is correctly localized following injection into *Xenopus* oocytes. *Nature* 336, 592–595.
- Zimniak, L., Dittrich, P., Gogarten, J.P., Kibak, H., and Taiz, L. (1988). The cDNA sequence of the 69-kD subunit of the carrot vacuolar H^+ -ATPase: homology to the β -chain of F_0F_1 -ATPases. *J. Biol. Chem.* 263, 9102–9112.